In situ fabrication of electrically conducting bacterial cellulose-polyaniline-titanium-dioxide composites with the immobilization of *Shewanella xiamenensis* and its application as bioanode in microbial fuel cell

Duy H. Truong[a,b], Mai S. Dam[b], Erika Bujna[a], Judit Rezessy-Szabo[a], Csilla Farkas[a], Vu Ngoc Ha Vi[a], Olivia Csernus[a], Vuong D. Nguyen[b], Nicholas Gathergood[c], László Friedrich[d], Mohamed Hafidi[e,f], Vijai Kumar Gupta[g,*] and Quang D. Nguyen[a,*]

[a] Research Centre for Bioengineering and Process Engineering, Faculty of Food Science, Szent István University, H-1118 Budapest, Ménesi út 45. Hungary.

[b] Institute of Food Technology and Biotechnology, Industrial University of Ho Chi Minh City, No. 12 Nguyen Van Bao, Ward 4, Go Vap District, Ho Chi Minh City, Viet Nam.

[c] School of Chemistry, University of Lincoln, Joseph Banks Laboratories, Green Lane, Lincoln, Lincolnshire LN6 7DL, UK.

[d] Research Centre for Food Technology, Faculty of Food Science, Szent István University, H-1118 Budapest, Ménesi út 45. Hungary.

[e] Laboratory of Microbial Biotechnologies, Agrosciences and Environment, Faculty of Sciences Semlalia, Cadi Ayyad University Marrakech, Morocco.

[f] Agrobiosciences Program, University Mohammed VI Polytechnic (UM6P), Lot 660, Hay Moulay Rachid, 43150, Ben Guerir, Morocco

[g] AgroBioSciences (AgBS) and Chemical & Biochemical Sciences (CBS), University Mohammed VI Polytechnic (UM6P), Lot 660, Hay Moulay Rachid, 43150, Benguerir – Morocco

* Corresponding authors: E-mail: Nguyen.Duc.Quang@etk.szie.hu (NDQ), vijaifzd@gmail.com (V.K.G.)

Abstract

The electrical conducting bacterial cellulose/polyaniline (BC/PANI) based composites were synthesized over *in situ* polymerization of aniline onto BC with ammonium-persulphate (APS) and chloride hexahydrate of iron (III) as oxidant ($FeCl_3.6H_2O$). The conductivity of synthesized BC was improved in the presence of a titanium-dioxide (TiO_2) coating. The conductivity of BC/PANI/TiO_2/APS was 3.7 S/m compare 2.9 S/m and 2.67 S/m with BC/PANI/TiO_2/$FeCl_3.6H_2O$ and BC/PANI/APS, respectively. Moreover, when using the BC/PANI/TiO_2/APS as anode with the immobilization of *Shewanella xiamenensis,* an improved efficiency of microbial fuel cell was observed. The power-density maximized 38.89 W/m^3 with BC/PANI/TiO_2/APS anode compared with 2.57 W/m^3 in the case of bare BC anode. These results will serve good base for the development of compact microbial fuel cell with high power density.

Keywords: bacteria cellulose/polyaniline/titanium-dioxide; *Shewanella xiamenensis*; microbial fuel cells; hydrogel bioanode; immobilization

1 Introduction

In recent years, alternative renewable energy systems have elicited great interest. Microbial fuel cell (MFC) can convert organic (biological) matter directly into energy [1-4], thus they are classified as renewable energy systems [5, 6]. In MFC, microorganisms biocatalyze the oxidation of organic matter and release electrons into the anodic electrode. Then, these electrons are transported to the cathodic electrode via the external circuit, resulting in a current generated. The organic compounds play a primary role as an electron source in microbial processes [7-10]. Many factors affect performance MFC such as microorganisms, substrate, mediator, electrode material etc. [11-13]. Electrodes are integral parts because of their key electron transfer role and research leading to enhanced efficiency of MFC [14] is

worthwhile. Electrode materials should have good electrical conductivity, biocompatibility, chemical stability, large surface area and mechanical strength [15-17]. Carbon materials with their high electric conductivity and stability are usually used in anode fabrication. However, besides carbon materials, other materials have been studied and used as anode materials in MFC [18].

Cellulose is a well-known non-toxic and low-cost polymer. It is also a naturally biocompatible polymer and has been used in many fields [19, 20]. Bacterial cellulose (BC) produced by fermentation of *Acetobacter* under static or agitated conditions and it is also classed as an exopolysaccharide. It has some outstanding characteristics compared to plant cellulose such as ultrafine network structure, higher purity, water retention capability, porosity, biological interaction and mechanical strength [21-23]. Chemically, BC is linear polysaccharide chains having glucose units linked together by β(1,4) glycosidic bounds, and intermolecular by hydrogen bonds. *Acetobacter* bacteria is considered as a strictly aerobic model bacteria species with high BC production capacity [24] and hydrogel cellulose will be formatted on the top surface of the liquid culture [25].

In recent years, conducting polymer-cellulose composites received significant interest due to high potentials in industrial applications, including as batteries, sensors and electrical devices. Polyaniline (PANI) has played a great role in energy storage, due to its controllable electrical conductivity, facile synthesis and availability as a low-cost material [26]. Besides other types of scaffolds based on cellulose (e.g. plant cellulose, cellulose derivatives and microcrystalline cellulose), bacterial cellulose membrane is an attractive cellulose scaffold for the preparation of conducting polymer-cellulose [23]. BC coated with conducting polymers is now well known as a new promising polymer [27]. BC/PANI is a typical example for BC combination and conducting polymer with the integration of several

properties such as tensile strength, biocompatibility, high surface areas and electrical conductivity [27, 28]. In addition, Wang et al. [23] have fabricated BC/PANI material with high electrical conductivity. In many types of research, the PANI coated anode was successfully used in the MFC to enhance power density [16, 29, 30]. Furthermore, the modification of PANI polymers with the supplement of titanium dioxide have significantly enhanced the current densities of MFC [31].

The main focus of the present study is *in situ* fabrication of electrically conducting bacterial cellulose/polyaniline/titanium-dioxide composites with the immobilization of *Shewanella xiamenensis* and its electrical performance in the microbial fuel cell.

2 Materials and methods

2.1 Microbial culture conditions

Shewanella xiamenensis DSMZ 22215 strain was obtained and maintained accordingly to Szöllősi et al. [6]. The bacterial cells from 24 h cultures in Luria-Bertani (LB) at 180 rpm were separated by centrifuge 10,000 rpm and used for immobilization.

2.2 Preparation of BC hydrogel

Acetobacter xylinum ATCC 23768 strain was used for bacteria cellulose production. Bacteria were cultivated on Schramm-Hestrin (SH) medium [32]. A single *Acetobacter xylinum* colony on SH agar medium was transferred into liquid SH medium. The cellulose sheets were shaped on the top-surface of the culture broth after 7 days at 28 ºC. The cellulose sheets with 0.5 cm thickness were removed and washed with deionized water, sodium dodecyl sulphate 2% and purified in NaOH 0.1N [33]. They were cut into 2 x 3 cm pieces

and sterilized before they were used for the fabrication of electrically conducting composites and cell immobilization.

2.3 Development of electrically conducting BC/PANI, BC/PANI/TiO_2 and bare BC composites

BC/PANI composites were made *in situ* oxidative polymerization of aniline by using ammonium persulphate (APS) called BC/PANI/APS or iron (III) chloride hexahydrate ($FeCl_3.6H_2O$) called BC/PANI/$FeCl_3.6H_2O$ as oxidant. For the preparation of BC/PANI composites, BC hydrogel membranes with 2 x 3 x 0.5 cm were cut and immersed in distilled water (1:10 w/v) and then aniline (Merck, Hungary) were added. In the first ultra-sonification process, the Clifton MU-8 sonicator at 40 kHz and 30 W performance was used for 2h; hydrogen bonding was formed allowing the monomer to assemble onto the BC surface. In the next step, the oxidant (ammonium-persulphate, Reanal, Hungary) or iron (III) chloride hexahydrate) was mixed. The BC was synthesized in the 2^{nd} ultra-sonication (40 kHz, 30 W) condition for 2h in the ice. After polymerization was started the colour of the solution changed to dark green from ivory in an overnight reaction. In the case of fabrication of electrically conducting BC/PANI/TiO_2 composites, TiO_2 (Sigma Aldrich) was mixed simultaneously with oxidants. For comparison, bare BC without aniline oxidative polymerization was used.

2.4 Immobilization of *Shewanella xiamenensis* into bare BC, BC/PANI and BC/PANI/TiO2 using adsorption method

The *Shewanella xiamenensis* cells in LB broth medium after 24 hours at 30 °C in incubator shaker 180 rpm were separated using the centrifugal method and suspended in isotonic saline phosphate-buffer (PBS, Sigma-Aldrich) to get cell number of 10^9 CFU/ml. Bare BC,

BC/PANI and BC/PANI/TiO_2 composite membranes were incubated in *Shewanella xiamenensis* suspension at 30^0C with shaking at 200 rpm from 12 – 96 hours. After that, composite membranes were washed 3 times with PBS to remove free cells.

2.5 Construction batch and a semi-continuous batch of MFC

Dual-chamber MFC was prepared with a similar volume of anode and cathode chamber (24 mL) and a Nafion 117 proton-exchange membrane was applied for separation of two chambers. The cathode chamber was filled with solution of 0.5 M of Sorensen phosphate buffer (pH = 7) contained 0.1 M of potassium-hexaferrocyanate. Bare BC, BC/PANI and BC/PANI/TiO_2 with immobilized bacteria cells act as an anode electrode and anode chamber was filled with modified LB medium that contains 10g/L glucose without agar. Graphite sheets with surface area 6 cm^2 as cathode were placed in the respective chambers. Generally, the external resistance with capacity of 500 Ω in parallel with a digital multimeter was used to connect the electrodes (Figure 1). Both batch and semi-continuous operation modes used for investigation of electric performance of MFC.

The voltage was continuously measured in the external resistance (500 Ω). The Ohm's law (I=V/R) was used to calculate the current (I) in MFC based on the electric voltage (V) and the external resistance (R). While the current density (P) of MFC was calculated according to equation P = I.V, whereas the power density (Pd) was obtained based on Pd = P/d, where d is the volume of bare BC or synthesized BC.

2.6 Bare BC, BC/PANI and BC/PANI/TiO_2 Characterization

2.6.1 Conductivity measurements

BC/PANI, BC/PANI/TiO_2 conductivity was analyzed with four-point probe technique. According to the four-point method, electrical resistance and electrical current were measured by a digital multimeter VC-830 (Voltcraft, Germany).

2.6.2 FT-IR

The infrared spectra of newly fabricated bare BC, BC/PANI and BC/PANI/TiO_2 composites were obtained on a JASCO-4700 infrared spectrometer using KBr pellets with a wavelength range of 4000 to 400 cm^{-1}.

2.6.3 Scanning electron microscope

Scanning electron microscope (SEM, JSM-6480LV-JED 2300, Jeol, Japan) was used to analyze the structure of the surface of bare BC, BC/PANI and BC/PANI/TiO_2.

2.6.4 Electrochemical measurements

Electrochemical characterization of bare BC and BC/PANI was performed by cyclic voltammetry (CV) techniques. Cyclic voltammetry (CV) was conducted using the open-source potentiostat (IO Rodeo, USA) with saturated calomel electrode (SCE) and platinum wire.

2.6.5 Cell number determination of immobilized *Shewanella xiamenensis*

The cell number of immobilized *Shewanella xiamenensis* in bare BC, BC/PANI and BC/PANI/TiO_2 were determined by plate count method on Marine agar (Scharlau, Spain). After immobilization of *Shewanella xiamenensis* cell, bare BC and synthesized BC were washed 3 times

with PBS and digested with the cellulase enzyme (Sigma, Aldrich). The grown colonies were counted after incubation for 24 hours, and the number of colonies was determined.

3 Results and discussions

3.1 Fabrication of electrically conducting composites from bacteria cellulose

The BC/PANI electrical conductivity composites was strongly dependent upon reaction conditions. The effect of preparation conditions (aniline concentration and $FeCl_3.6H_2O$, ammonium persulfate) on the BC/PANI nanocomposites conductivity was investigated using the Central Composite Design (CCD) of response surface method (Figure 2). The BC/PANI electrical conductivity increased when the aniline, $FeCl_3.6H_2O$ and ammonium persulfate concentration increased. The maximum BC/PANI composites conductivity could be attained when prepared as follows: concentration of aniline 0.2 mol/L; molar ratio of ammonium-persulfate:aniline 1.2:1; molar ratio of $FeCl_3.6H_2O$:aniline 1.5:1; reaction temperature 0 – 5 ^oC; polymerization reaction time 14 hours for the completion of polymerization. The conductivity of BC/PANI/APS composites obtained was 2.67 S/m and with BC/PANI/$FeCl_3.6H_2O$ composites 2.29 S/m.

Figure 3 illustrates the effect of TiO_2 concentration on the conductivity of BC/PANI/TiO_2 composites. The maximum conductivity of BC/PANI/APS was 3.7 S/m when prepared at 0.3 mol/L TiO_2 concentration and for BC/PANI/$FeCl_3.6H_2O$ was 2.9 S/m with 0.2 mol/L TiO_2.

Infrared spectra of bare BC and synthesized BC composites were measured by FT-IR to evaluate chemical structure (Figure 4) The FT-IR spectrum of pure BC presented broad absorption band of 3200 - 3550 cm^{-1}, assigned H-bond for -OH [23, 34-36]. The peak at 2895 cm^{-1} showed the aliphatic C-H stretching vibration. In the case of BC/PANI

composite, the stretching vibration of quinoid and benzenoid rings structure was at peaks 1556 and 1470 cm^{-1}, respectively. C-O-C stretching vibrations of the pyranose skeletal ring were at the range of 1060-1030 cm^{-1} [23]. The FT-IR spectra of BC/PANI/TiO_2 composite showed an absorption band at 637 cm^{-1}. This feature supports our claims that an interaction between TiO_2 and the hydroxyl group of cellulose occurred [37] and that the BC was sufficiently coated by PANI and TiO_2.

The surface characteristics of bare BC, BC/PANI and BC/PANI/TiO_2 were evaluated by SEM images at x1000 magnification (Figure 5). The morphologies are particularly different between bare BC and BC/PANI. In the case of bare BC, a smooth surface with featureless morphology was observed (Figure 5a). In comparison, the surface of BC/PANI was rough and covered with materials (Figure 5b-d). The surface structure of BC/PANI/TiO_2 showed the particles entangled with cellulose and PANI particles, present a much denser structure (Figure 5c, d). This result showed that the BC coating adhered to the cellulose and formed a continuous conducting network for the high electrical conductivity [23, 38, 39].

3.2 Electrical performance of the bare BC and synthesized BC bioanodes

3.2.1 Immobilization *Shewanella xiamenensis* to form the bioanode

Shewanella xiamenensis was immobilized in bare BC, BC/PANI and BC/PANI/TiO_2 composites. Figure 6 shows effect of incubation conditions on the immobilized cell numbers. In the case of bare BC, the cell number increased until 36 hours whereupon a stable value was observed for a further 36 hours (1.2×10^6 CFU/g). After 48 hours of immobilization microorganisms on all BC/PANI and BC/PANI/TiO_2 electrodes had reached their maximum cell numbers and were stable for a further 24h. The maximum cell number of BC/PANI/TiO_2 using ammonium persulphate and $FeCl_3.6H_2O$ as oxidant was

212 1.2 x 10^6 CFU/g and 1.1 x 10^6 CFU/g, respectively. When the immobilization process was
213 completed, the bare BC, BC/PANI, BC/PANI/TiO_2 were covered by sodium alginate film.
214 The ability to immobilize microorganisms into bare BC has been previously described [33].
215
216 **3.2.2 Electrical performance of different bioanodes**
217 Five types of bioanodes namely bare BC, BC/PANI/$FeCl_3.6H_2O$, BC/PANI/APS,
218 BC/PANI/TiO_2/$FeCl_3.6H_2O$ and BC/PANI/TiO_2/APS with the immobilization *Shewanella*
219 *xiamenensis* were used in different MFC systems MFC1, MFC2, MFC3, MFC4, MFC5,
220 respectively. The membrane was 2x3x0.5 cm and the immobilization cell numbers were
221 counted to be in the range 1.1 – 1.2 x 10^6 CFU. The voltage in MFC was counted with 500
222 Ohm and the MFC was operated until the electric voltage outputted to near zero (out of
223 substrate). The power density of all MFC system is illustrated in Figure 7.
224 The power density rapidly increased in MFC with BC/PANI/TiO_2 anode (MFC4 and
225 MFC5) compared with the control system bare BC (MFC1). The power density of MFC5
226 reached the maximum value (38.89 W/m^3) after 8h of operation and maintained this power
227 density for 28h. The power density of MFC5 was 15-fold higher than MFC1 with bare BC
228 anode (2.57 W/m^3). MFC1 got a maximum value (7.09 W/m^3) after 16 hours of operation.
229 In the case of BC/PANI/TiO_2 (MFC4) using $FeCl_3.6H_2O$ as an oxidant – the power density
230 value peaked around 23.95 - 29.30 W/m^3, lower than MFC5. MFC2 and MFC3 also showed
231 lower power density values in comparison with MFC4 and MFC5. The combination of
232 BC/PANI and TiO_2 contributed to the increase in power density. Taşkan et al. [40] used a
233 Ti-TiO_2 electrode to enhance the electricity generation in MFC and their research showed
234 that the current density achieved 15-fold higher than the carbon-based electrode. Also, in
235 2013, Wu et al. [41] successfully fabricated the carbon nanotube-gold-titanium-dioxide

236 (CNT/Au/TiO_2) that has nanostructure, and it was applied as modified anode in the MFC.
237 They reported that the power density was 3-fold higher than the bare carbon paper electrode.
238 Indeed, due to the number of technological and economical advantages such as large in
239 surface area, low cost and high conductivity, the conducting polymers can serve very good
240 materials for formation of anodic electrode in MFC. For example, Szöllősi et al. [6]
241 successfully fabricated an alginate/PANI/TiO_2/graphite composite for MFC application and
242 they reported that the MFC with this anode has significantly high electrical conductivity
243 and power density as well as exhibited good stability. Li et al. [42] also used modified
244 carbon felt electrodes with four classes of conducting polymers namely polyaniline,
245 poly(aniline-co-aminophenol), poly(aniline-co-2,4-diaminophenol) (PANDAP) and
246 poly(aniline-1,8 diaminonaphthalene) (PANDAN). Their method enhanced the power
247 densities by 300% and 180% for abiotic cathodes and biocathodes, respectively, compared
248 to unmodified carbon felts electrodes.
249 To consider the effectiveness of BC/PANI/TiO_2/APS with immobilization of *Shewanella*
250 *xiamenensis*, semi-continuous batch was set-up after voltage output of MFC5 decreased.
251 The anode chamber of MFC5 was fed with fresh substrate and the performance is shown in
252 Figure 8. Maximum power density of each cycle peaked around 35.81 W/m^3 after 30^{th}
253 hours. In this result, MFC still maintains the ability to produce electricity if the nutritional
254 medium is met. The cycle time of MFC takes about 70-72 hours from the fresh feeding
255 medium to exhaust of glucose. Several authors also reported the increase in power density
256 of MFC using modified anode with supplement of polyaniline (Table 1). Additionally, in
257 the case of modified anode coated by TiO_2, the power output of the MFC using
258 BC/PANI/TiO_2 was higher (2.26-fold) and (3.94-fold) than that of the graphite

sheets/polyaniline/graphene/TiO_2 and alginate/polyaniline/TiO_2/graphite, respectively [6, 45].

The MFC performance is typically predictable by the polarization curve [43]. The polarization curve of MFC5 was measured and shown in Figure 9. The maximum power density of MFC5 system was 40.66 W/m^3 with a current density of 116.72 A/m^3. The power overshoot of MFC5 was absent. It can be explained by high anodic capacitance, and high density of cells in the anode. Generally, in the MFC, the power overshoot may be caused by the immature biofilm on the anode electrode or the lack of anodic capacitance. These results clearly substantiate the suitability of using BC/PANI/TiO_2/APS as anode for MFC. Cyclic voltammetry (CV) is extensively used to consider the extracellular electron transfer processes in MFC. This method was used to investigate the catalytic and capacitive behavior of different bioelectrodes [43]. The CV response of MFC5 with BC/PANI/TiO_2/APS composite anode was measured. The redox peaks were found for the systems of BC/PANI/TiO_2 anode composite (Figure 10). The oxidation and reduction peaks were 0.2V and -0.07 V, respectively. This result affirmed that c-type cytochromes were involved in the electron transfer process [44] and successful fabrication of BC/PANI/TiO_2 was confirmed.

4 Conclusion

The electrical conducting BC/PANI composites were successfully fabricated by *in situ* polymerization of self-assembled aniline onto BC with ammonium-persulphate or $FeCl_3.6H_2O$ as oxidant. The reaction conditions such as aniline concentration and concentration of oxidant have strength effects on the conductivity of conducting polymers. In addition, the use of ammonium-persulphate as an oxidant showed significant enhancement in increasing conductivity of BC/PANI compared with using $FeCl_3.6H_2O$. The

283 fabrication of BC/PANI composites with a covering of TiO_2 were successful with a
284 significant increase in conductivity. The BC/PANI/TiO_2 anode system was suitable for
285 improving the efficiency of the MFC. Moreover, the fabrication of BC/PANI and
286 BC/PANI/TiO_2 composites with the immobilization bacteria cell and as a new bio-anode
287 was developed. By applying the BC/PANI/TiO_2/APS bio-anode, the maximum power
288 density of MFC was about 15-fold higher than that of bare BC. The BC/PANI and
289 BC/PANI/TiO_2 bio-anode improved the transport of electron from bacterium cells to anode.
290 Furthermore, this study provided an economical anode material because of its reusability
291 and cheapness.
292

293 **Author Contributions**

294 Q.D.N. and V.K.G. developed the concept and led the design of experiments as well as correction
295 of the manuscript; D.H.T., M.S.D., V.N.H.V., Cs.F., J.M.R-Sz, E.B., O.Cs., V.D.N., L.F., designed
296 and carried out experiments, collected data as well as wrote the draft of the manuscript; N.G. and
297 M.H. were scientific advisors for concept development and experimental design as well as
298 correction of manuscript.

299 **Conflicts of interest**

300 There are no conflicts to declare.

301 **Acknowledgements**

302 This work is supported by the New Széchényi Plant Project No. EFOP-3.6.3.-VEKOP-16-
303 2017-00005 as well as by Doctoral School of Food Science, Szent Istvan University, and
304 by the Higher Education Institutional Excellence Program (Project No. 20430-
305 3/2018/FEKUTSTRAT) awarded by the Ministry of Human Capacities. VKG and NG

306 would like to acknowledge the EU 7th Framework Programme for research, technological
307 development, and demonstration activities under grant agreement No. 621364 (TUTIC-
308 Green). QDN received Bolyai Research Grant from the Hungarian Academic of Sciences.
309

References

[1] Choudhury P, Ray RN, Bandyopadhyay TK, Bhunia B. Fed batch approach for stable generation of power from dairy wastewater using microbial fuel cell and its kinetic study. Fuel. 2020;266:117073. https://doi.org/10.1016/j.fuel.2020.117073

[2] Divya Priya A, Pydi Setty Y. Cashew apple juice as substrate for microbial fuel cell. Fuel. 2019;246:75-8. https://doi.org/10.1016/j.fuel.2019.02.100

[3] Naina Mohamed S, Thomas N, Tamilmani J, Boobalan T, Matheswaran M, Kalaichelvi P, et al. Bioelectricity generation using iron(II) molybdate nanocatalyst coated anode during treatment of sugar wastewater in microbial fuel cell. Fuel. 2020;277:118119. https://doi.org/10.1016/j.fuel.2020.118119

[4] Thulasinathan B, Nainamohamed S, Ebenezer Samuel JO, Soorangkattan S, Muthuramalingam J, Kulanthaisamy M, et al. Comparative study on Cronobacter sakazakii and Pseudomonas otitidis isolated from septic tank wastewater in microbial fuel cell for bioelectricity generation. Fuel. 2019;248:47-55. https://doi.org/10.1016/j.fuel.2019.03.060

[5] Palanisamy G, Jung H-Y, Sadhasivam T, Kurkuri MD, Kim SC, Roh S-H. A comprehensive review on microbial fuel cell technologies: Processes, utilization, and advanced developments in electrodes and membranes. Journal of Cleaner Production. 2019;221:598-621. https://doi.org/10.1016/j.jclepro.2019.02.172

[6] Szöllősi A, Hoschke Á, Rezessy-Szabó JM, Bujna E, Kun S, Nguyen QD. Formation of novel hydrogel bio-anode by immobilization of biocatalyst in alginate/polyaniline/titanium-dioxide/graphite composites and its electrical performance. Chemosphere. 2017;174:58-65. https://doi.org/10.1016/j.chemosphere.2017.01.095

[7] Kumar SS, Kumar V, Malyan SK, Sharma J, Mathimani T, Maskarenj MS, et al. Microbial fuel cells (MFCs) for bioelectrochemical treatment of different wastewater streams. Fuel. 2019;254:115526. https://doi.org/10.1016/j.fuel.2019.05.109

[8] Prestigiacomo C, Fernandez-Marchante CM, Fernández-Morales FJ, Cañizares P, Scialdone O, Rodrigo MA. New prototypes for the isolation of the anodic chambers in microbial fuel cells. Fuel. 2016;181:704-10. https://doi.org/10.1016/j.fuel.2016.04.122

[9] Subha C, Kavitha S, Abisheka S, Tamilarasan K, Arulazhagan P, Rajesh Banu J. Bioelectricity generation and effect studies from organic rich chocolaterie wastewater using continuous upflow anaerobic microbial fuel cell. Fuel. 2019;251:224-32. https://doi.org/10.1016/j.fuel.2019.04.052

[10] Wang H, Wang Q, Li X, Wang Y, Jin P, Zheng Y, et al. Bioelectricity generation from the decolorization of reactive blue 19 by using microbial fuel cell. Journal of Environmental Management. 2019;248:109310. https://doi.org/10.1016/j.jenvman.2019.109310

[11] Karthick S, Haribabu K. Bioelectricity generation in a microbial fuel cell using polypyrrole-molybdenum oxide composite as an effective cathode catalyst. Fuel. 2020;275:117994. https://doi.org/10.1016/j.fuel.2020.117994

[12] Kumar SS, Kumar V, Kumar R, Malyan SK, Pugazhendhi A. Microbial fuel cells as a sustainable platform technology for bioenergy, biosensing, environmental monitoring, and other low power device applications. Fuel. 2019;255:115682. https://doi.org/10.1016/j.fuel.2019.115682

[13] Luo H, Yu S, Liu G, Zhang R, Teng W. Effect of in-situ immobilized anode on performance of the microbial fuel cell with high concentration of sodium acetate. Fuel. 2016;182:732-9. https://doi.org/10.1016/j.fuel.2016.06.032

[14] Huggins T, Wang H, Kearns J, Jenkins P, Ren ZJ. Biochar as a sustainable electrode material for electricity production in microbial fuel cells. Bioresource Technology. 2014;157:114-9. https://doi.org/10.1016/j.biortech.2014.01.058

[15] Aelterman P, Rabaey K, Pham HT, Boon N, Verstraete W. Continuous electricity generation at high voltages and currents using stacked microbial fuel cells. Environmental Science and Technology. 2006;40:3388-94. https://doi.org/10.1021/es0525511

[16] Logan BE, Hamelers B, Rozendal R, Schröder U, Keller J, Freguia S, et al. Microbial fuel cells: Methodology and technology. Environmental Science and Technology. 2006;40:5181-92. https://doi.org/10.1021/es0605016

[17] Schröder U. Anodic electron transfer mechanisms in microbial fuel cells and their energy efficiency. Physical Chemistry Chemical Physics. 2007;9:2619-29. https://doi.org/10.1039/b703627m

[18] Logan BE. Materials. Microbial Fuel Cells: John Wiley & Sons; 2007. p. 61-84.

[19] Bassas-Galia M, Follonier S, Pusnik M, Zinn M. 2 - Natural polymers: A source of inspiration. In: Perale G, Hilborn J, editors. Bioresorbable Polymers for Biomedical Applications: Woodhead Publishing; 2017. p. 31-64.

[20] He W, Benson R. 5 - Polymeric Biomaterials. In: Ebnesajjad S, editor. Handbook of Biopolymers and Biodegradable Plastics. Boston: William Andrew Publishing; 2013. p. 87-107.

[21] Dayal MS, Goswami N, Sahai A, Jain V, Mathur G, Mathur A. Effect of media components on cell growth and bacterial cellulose production from Acetobacter aceti MTCC 2623. Carbohydrate Polymers. 2013;94:12-6. https://doi.org/10.1016/j.carbpol.2013.01.018

[22] Vandamme EJ, De Baets S, Vanbaelen A, Joris K, De Wulf P. Improved production of bacterial cellulose and its application potential. Polymer Degradation and Stability. 1998;59:93-9. https://doi.org/10.1016/S0141-3910(97)00185-7

[23] Wang H, Zhu E, Yang J, Zhou P, Sun D, Tang W. Bacterial cellulose nanofiber-supported polyaniline nanocomposites with flake-shaped morphology as supercapacitor electrodes. The Journal of Physical Chemistry C. 2012;116:13013-9. https://doi.org/10.1021/jp301099r

[24] Lin D, Lopez-Sanchez P, Li R, Li Z. Production of bacterial cellulose by Gluconacetobacter hansenii CGMCC 3917 using only waste beer yeast as nutrient source. Bioresource Technology. 2014;151:113-9. https://doi.org/10.1016/j.biortech.2013.10.052

[25] Zhang H, Xu X, Chen C, Chen X, Huang Y, Sun D. In situ controllable fabrication of porous bacterial cellulose. Materials Letters. 2019;249:104-7. https://doi.org/10.1016/j.matlet.2019.04.026

[26] Pyarasani RD, Jayaramudu T, John A. Polyaniline-based conducting hydrogels. Journal of Materials Science. 2019;54:974-96. https://doi.org/10.1007/s10853-018-2977-x

[27] Li M, Guo Y, Wei Y, MacDiarmid AG, Lelkes PI. Electrospinning polyaniline-contained gelatin nanofibers for tissue engineering applications. Biomaterials. 2006;27:2705-15. https://doi.org/10.1016/j.biomaterials.2005.11.037

[28] Kamalesh S, Tan P, Wang J, Lee T, Kang ET, Wang C-H. Biocompatibility of electroactive polymer in tissue. Journal of biomedical materials research. 2001;52:467-78. https://doi.org/10.1002/1097-4636(20001205)52:33.0.CO;2-6

[29] Lai B, Tang X, Li H, Du Z, Liu X, Zhang Q. Power production enhancement with a polyaniline modified anode in microbial fuel cells. Biosensors and Bioelectronics. 2011;28:373-7. https://doi.org/10.1016/j.bios.2011.07.050

[30] Schröder U, Nießen J, Scholz F. A generation of microbial fuel cells with current outputs boosted by more than one order of magnitude. Angewandte Chemie - International Edition. 2003;42:2880-3. https://doi.org/10.1002/anie.200350918

[31] Watanabe K. Recent Developments in Microbial Fuel Cell Technologies for Sustainable Bioenergy. Journal of Bioscience and Bioengineering. 2008;106:528-36. https://doi.org/10.1263/jbb.106.528

403 [32] Kimura S, Chen H, Saxena I, Brown R, Itoh T. Localization of c-di-GMP-Binding Protein
404 with the Linear Terminal Complexes of Acetobacter xylinum. Journal of bacteriology.
405 2001;183:5668-74. https://doi.org/10.1128/JB.183.19.5668-5674.2001
406 [33] Fijałkowski K, Peitler D, Rakoczy R, Żywicka A. Survival of probiotic lactic acid bacteria
407 immobilized in different forms of bacterial cellulose in simulated gastric juices and bile salt
408 solution. LWT - Food Science and Technology. 2015;68. https://doi.org/10.1016/j.lwt.2015.12.038
409 [34] Jahan MS, Saeed A, He Z, Ni Y. Jute as raw material for the preparation of microcrystalline
410 cellulose. Cellulose. 2011;18:451-9. https://doi.org/10.1007/s10570-010-9481-z
411 [35] Sun R, Sun XF, Liu GQ, Fowler P, Tomkinson J. Structural and physicochemical
412 characterization of hemicelluloses isolated by alkaline peroxide from barley straw. Polymer
413 International. 2002;51:117-24. https://doi.org/10.1002/pi.815
414 [36] Wan Y, Wang J, Gama M, Guo R, Zhang Q, Zhang P, et al. Biofabrication of a novel
415 bacteria/bacterial cellulose composite for improved adsorption capacity. Composites Part A:
416 Applied Science and Manufacturing. 2019;125:105560.
417 https://doi.org/10.1016/j.compositesa.2019.105560
418 [37] Afsharpour M, Rad FT, Malekian H. New cellulosic titanium dioxide nanocomposite as a
419 protective coating for preserving paper-art-works. Journal of Cultural Heritage. 2011;12:380-3.
420 https://doi.org/10.1016/j.culher.2011.03.001
421 [38] Lv P, Feng Q, Wang Q, Li D, Zhou J, Wei Q. Preparation of bacterial cellulose/carbon
422 nanotube nanocomposite for biological fuel cell. Fibers and Polymers. 2016;17:1858-65.
423 https://doi.org/10.1007/s12221-016-6337-7
424 [39] Müller D, Mandelli J, Marins J, Soares B, Porto L, Rambo C, et al. Electrically conducting
425 nanocomposites: Preparation and properties of polyaniline (PAni)-coated bacterial cellulose
426 nanofibers (BC). Cellulose. 2012;19. https://doi.org/10.1007/s10570-012-9754-9

427 [40] Taşkan E, Hasar H, Ozkaya B. Usage of Ti-TiO2 electrode in microbial fuel cell to enhance
428 the electricity generation and its biocompatibility. Applied Mechanics and Materials.
429 2013;404:371-6. https://doi.org/10.4028/www.scientific.net/AMM.404.371
430 [41] Wu D, Xing D, Lu L, Wei M, Liu B, Ren N. Ferric iron enhances electricity generation by
431 Shewanella oneidensis MR-1 in MFCs. Bioresource Technology. 2013;135:630-4.
432 https://doi.org/10.1016/j.biortech.2012.09.106
433 [42] Li C, Ding L, Cui H, Zhang L, Xu K, Ren H. Application of conductive polymers in biocathode
434 of microbial fuel cells and microbial community. Bioresource Technology. 2012;116:459-65.
435 https://doi.org/10.1016/j.biortech.2012.03.115
436 [43] Pandit S, Khilari S, Roy S, Pradhan D, Das D. Improvement of power generation using
437 Shewanella putrefaciens mediated bioanode in a single chambered microbial fuel cell: Effect of
438 different anodic operating conditions. Bioresource Technology. 2014;166:451-7.
439 https://doi.org/10.1016/j.biortech.2014.05.075
440 [44] Zhang P, Liu J, Qu Y, Feng Y. Enhanced Shewanella oneidensis MR-1 anode performance by
441 adding fumarate in microbial fuel cell. Chemical Engineering Journal. 2017;328:697-702.
442 https://doi.org/10.1016/j.cej.2017.07.008
443 [45] Han TH, Parveen N, Shim JH, Nguyen ATN, Mahato N, Cho MH. Ternary Composite of
444 Polyaniline Graphene and TiO2 as a Bifunctional Catalyst to Enhance the Performance of Both the
445 Bioanode and Cathode of a Microbial Fuel Cell. Industrial & Engineering Chemistry Research.
446 2018;57:6705-13. https://doi.org/10.1021/acs.iecr.7b05314
447 [46] Qiao Y, Li CM, Bao S-J, Bao Q-L. Carbon nanotube/polyaniline composite as anode material
448 for microbial fuel cells. Journal of Power Sources. 2007;170:79-84.
449 https://doi.org/10.1016/j.jpowsour.2007.03.048

[47] Xu H, Wang L, Wen Q, Chen Y, Qi L, Huang J, et al. A 3D porous NCNT sponge anode modified with chitosan and Polyaniline for high-performance microbial fuel cell. Bioelectrochemistry. 2019;129:144-53. https://doi.org/10.1016/j.bioelechem.2019.05.008

455

456 Table 1. The power density of different polyaniline modified anode materials in the MFC

Anode material	MFC contruction	Bacteria	Substrate	P_{max} (W/m^3)	References
Alginate/polyaniline/ TiO_2/graphite	DCMFC	*Shewanella algae*	Glucose	9.86	[6]
Carbon nanotube/ polyaniline	-	*E. Coli*	Glucose	42*	[46]
Carbon cloth/polyaniline	DCMFC	-	Sodium acetate	5.16	[29]
Chitosan-nitrogen/ carbon nanotubes/ polyaniline	DCMFC	-	Sodium acetate	4.2	[47]
Graphite sheets/ polyaniline/graphene/TiO_2	DCMFC	*Shewanella oneidensis*	LB	79.3*	[45]
Bacteria cellulose/ polyaniline	DCMFC	*Shewanella xiamenensis*	Glucose	29.31 (137.4*)	This work
Bacteria cellulose/ polyaniline/TiO_2	DCMFC	*Shewanella xiamenensis*	Glucose	38.89 (179.4*)	This work

457 * mW/m^2; DCMFC: dual-chamber MFC

458

459 **Figure captions**

460 Figure 1. Schematic construction of dual-chamber MFC using BC, BC/PANI,
461 BC/PANI/TiO_2 composites as anode

462 Figure 2. Effect of reaction conditions (aniline concentration and ammonium persulfate,
463 $FeCl_3.6H_2O$) on the conductivity of BC/PANI composites: (a) BC/PANI/APS; (b)
464 BC/PANI/$FeCl_3.6H_2O$

465 Figure 3. Effect of titanium dioxide concentration in fabrication of BC/PANI/TiO_2
466 composites process on its conductivity: (a) BC/PANI/APS; (b) BC/PANI/$FeCl_3.6H_2O$

467 Figure 4. FT-IR spectra of bare BC, BC/PANI and BC/PANI/TiO_2 using ammonium
468 persulfate as oxidant

469 Figure 5. SEM images of (a) Bare BC, (b) BC/PANI/APS, (c) BC/PANI/TiO_2/APS, (d)
470 BC/PANI/TiO_2/$FeCl_3.6H_2O$

471 Figure 6. The number of immobilized *Shewanella xiamenensis* cells (CFU/g BC) in bare
472 BC, BC/PANI and BC/PANI/TiO_2 by adsorption-incubation method

473 Figure 7. The power density of MFC with different synthesized BC anode in a simple batch

474 Figure 8. The power density of MFC with BC/PANI/TiO_2/APS anode composite in semi-
475 continuous batch ("↓" indicate the new feeding cycle)

476 Figure 9. Polarization curve of MFC with BC/PANI/TiO_2/APS anode composite

477 Figure 10. Cyclic voltammogram for MFC using BC/PANI/TiO_2/APS anode with potential (vs
478 SCE)

479

480

481 Figure 1

482

483

484

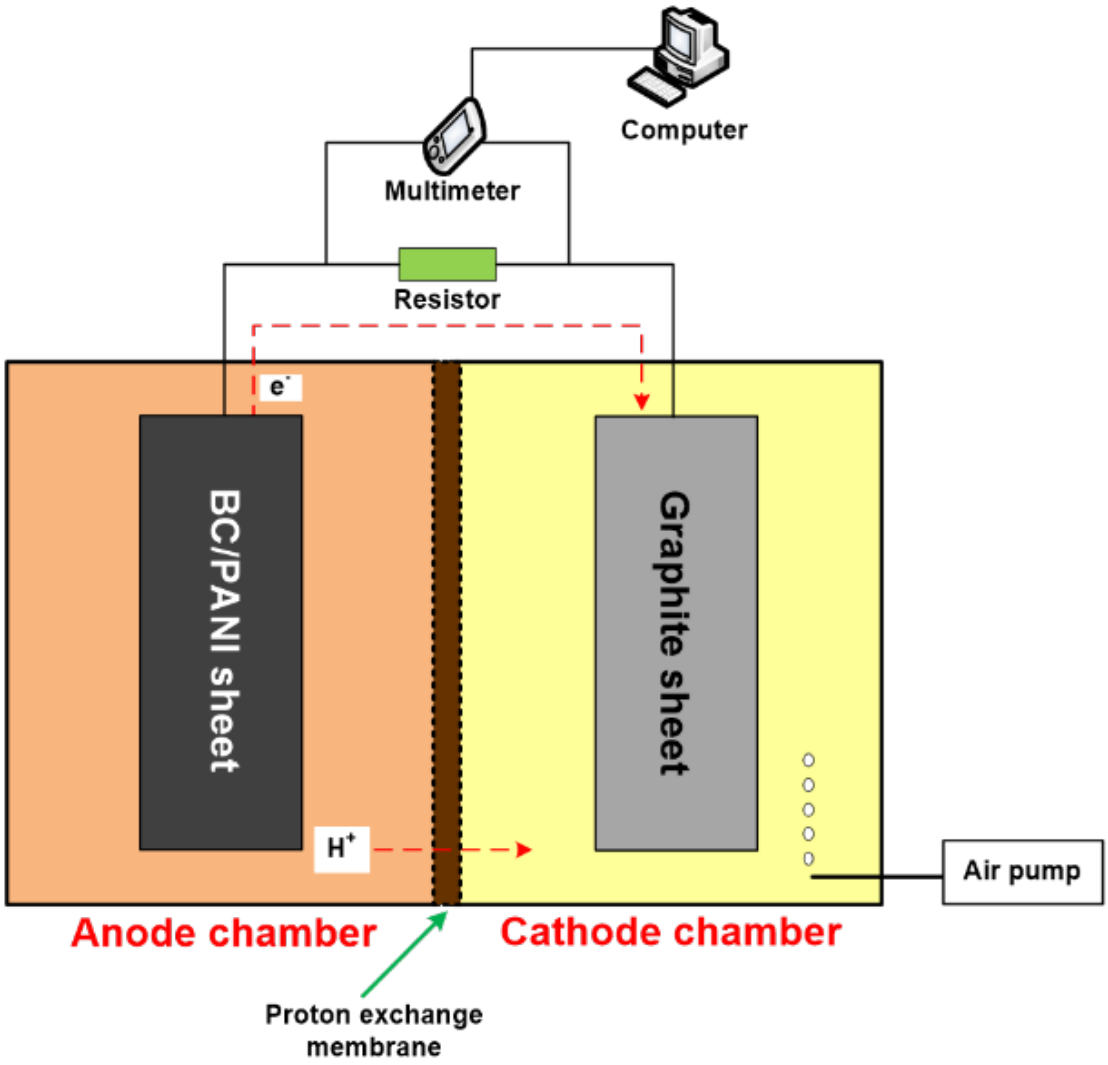

485

486

487

488

489

490 Figure 2

491

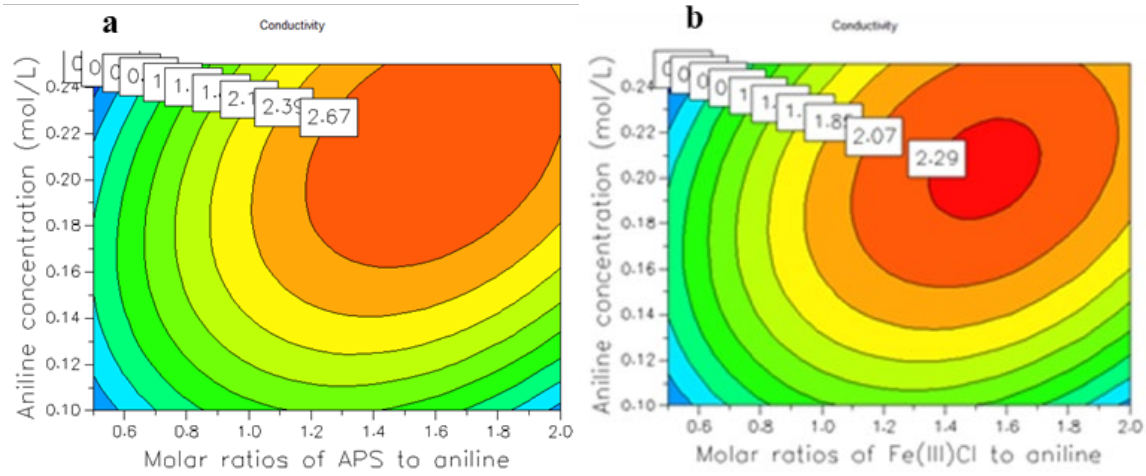

492

493

494

495 Figure 3

496

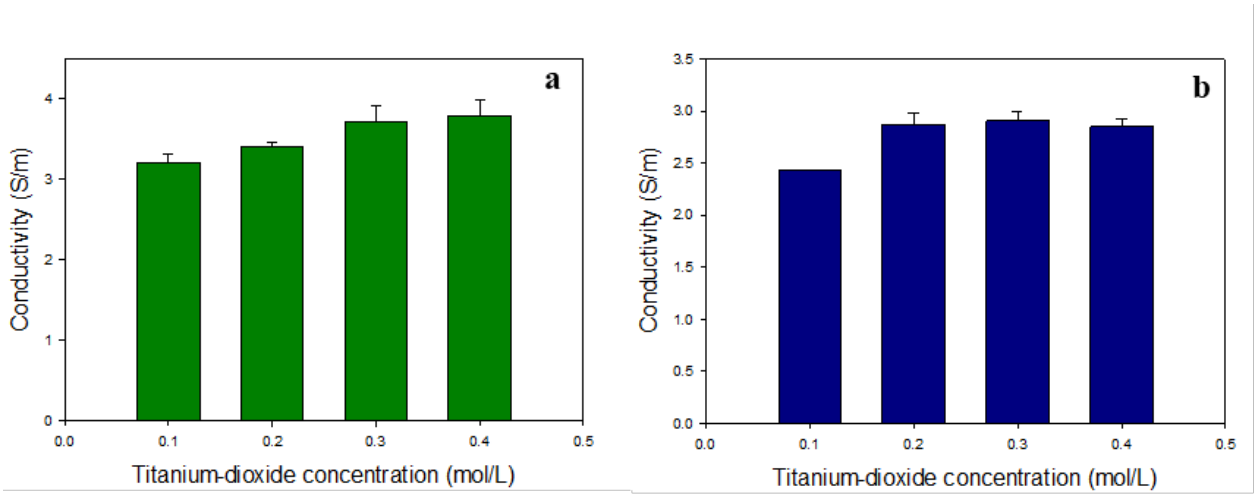

497

498

499

500

501 Figure 4

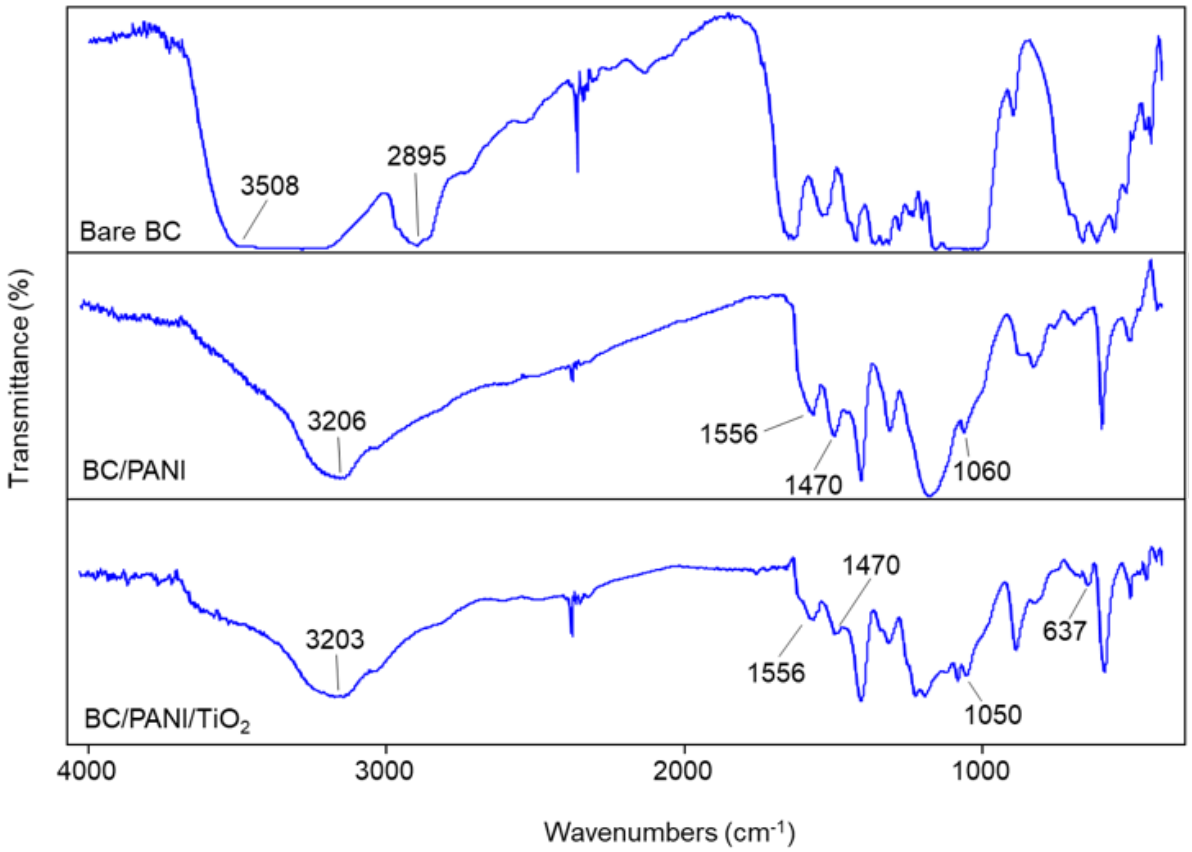

502

503

504

505

506 Figure 5

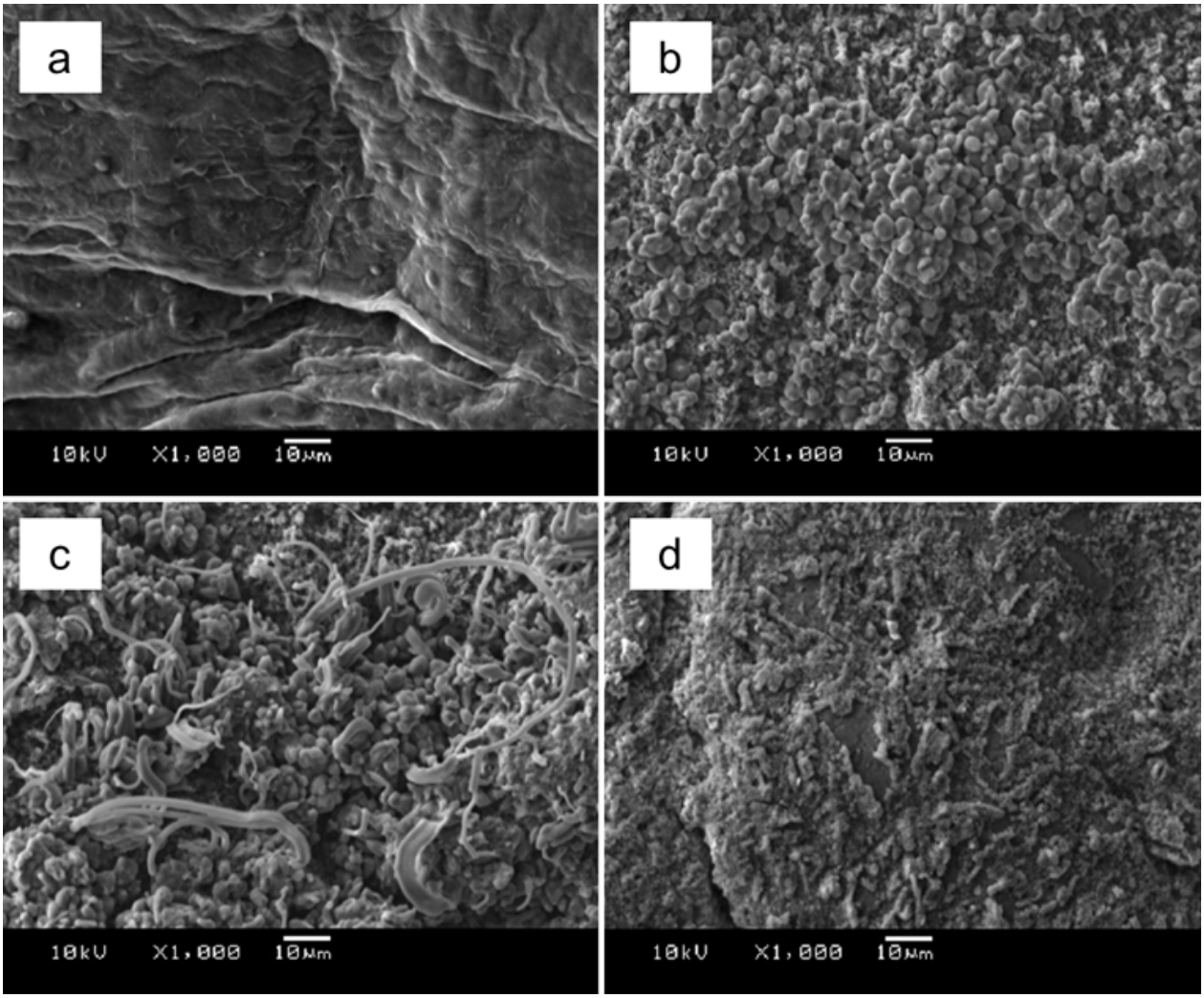

507

508

509

510 Figure 6

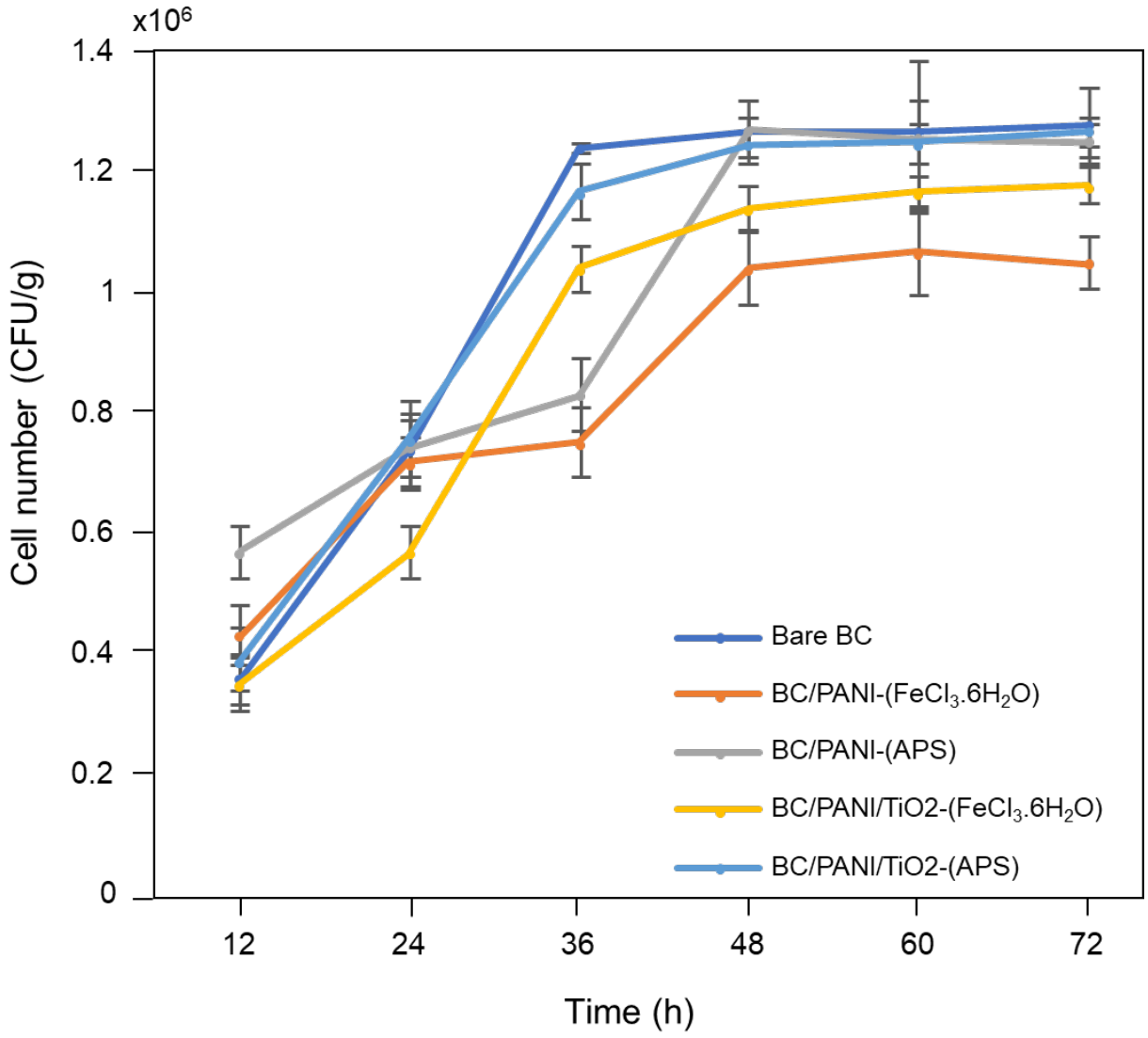

511

512

513

514

515 Figure 7

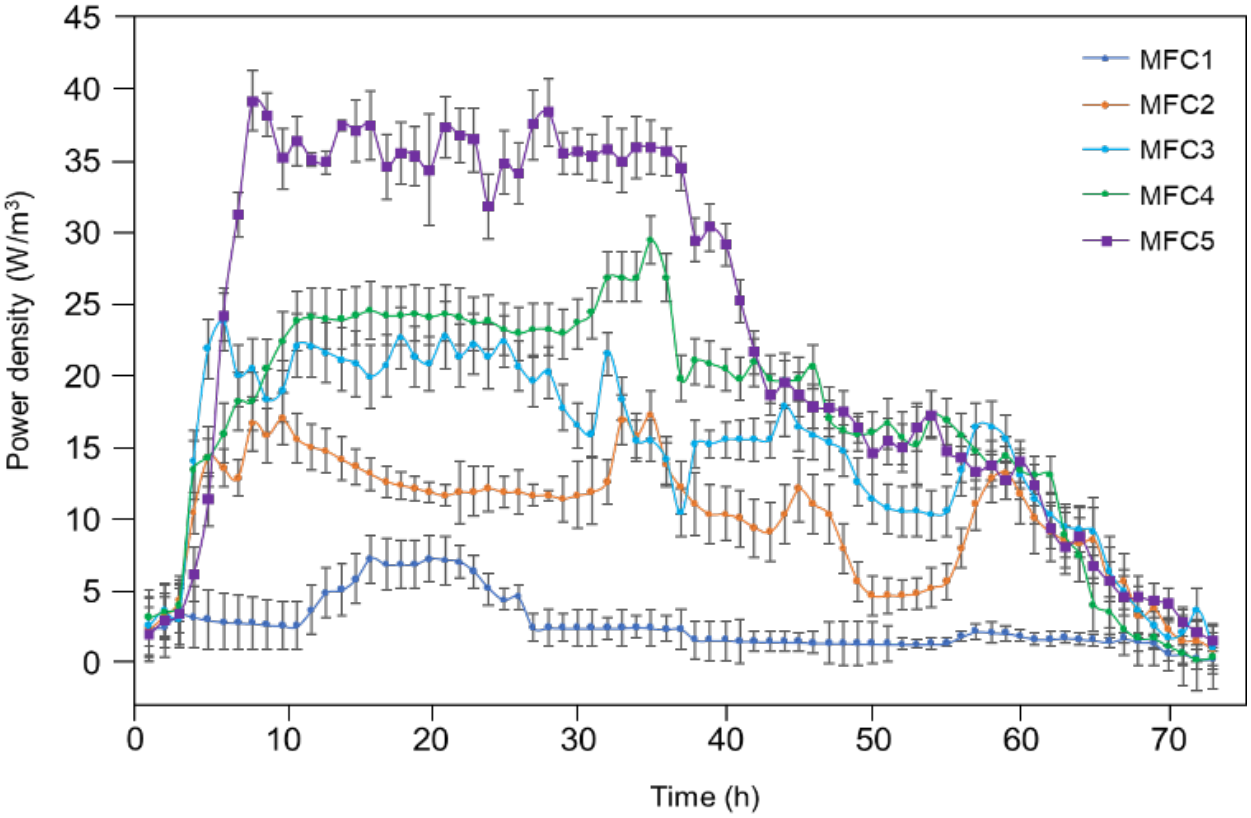

516

517

518 Figure 8

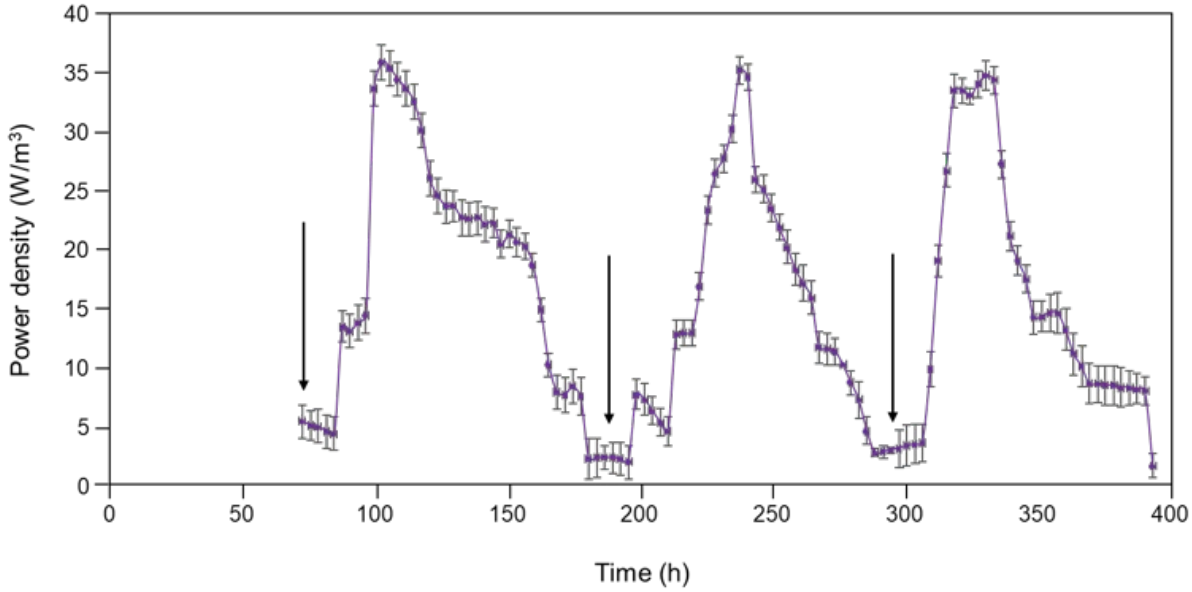

519

520

521

522 Figure 9

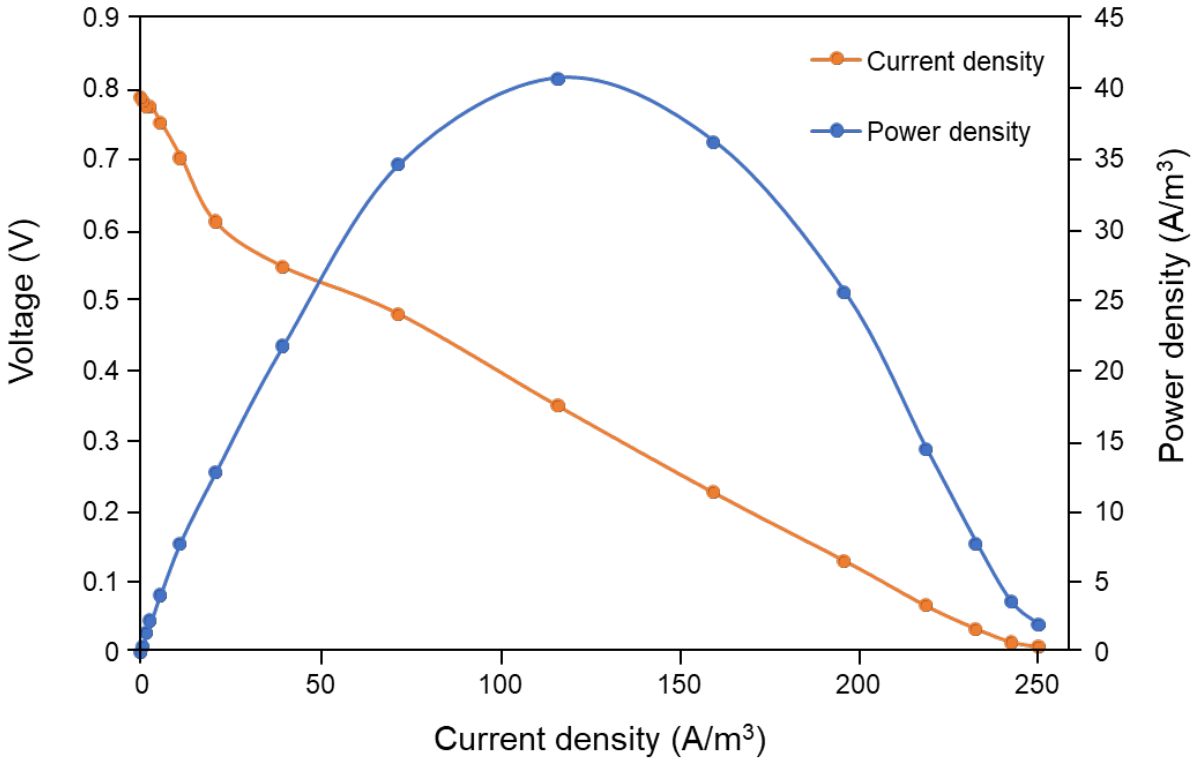

523

524

525

526

527 Figure 10

528

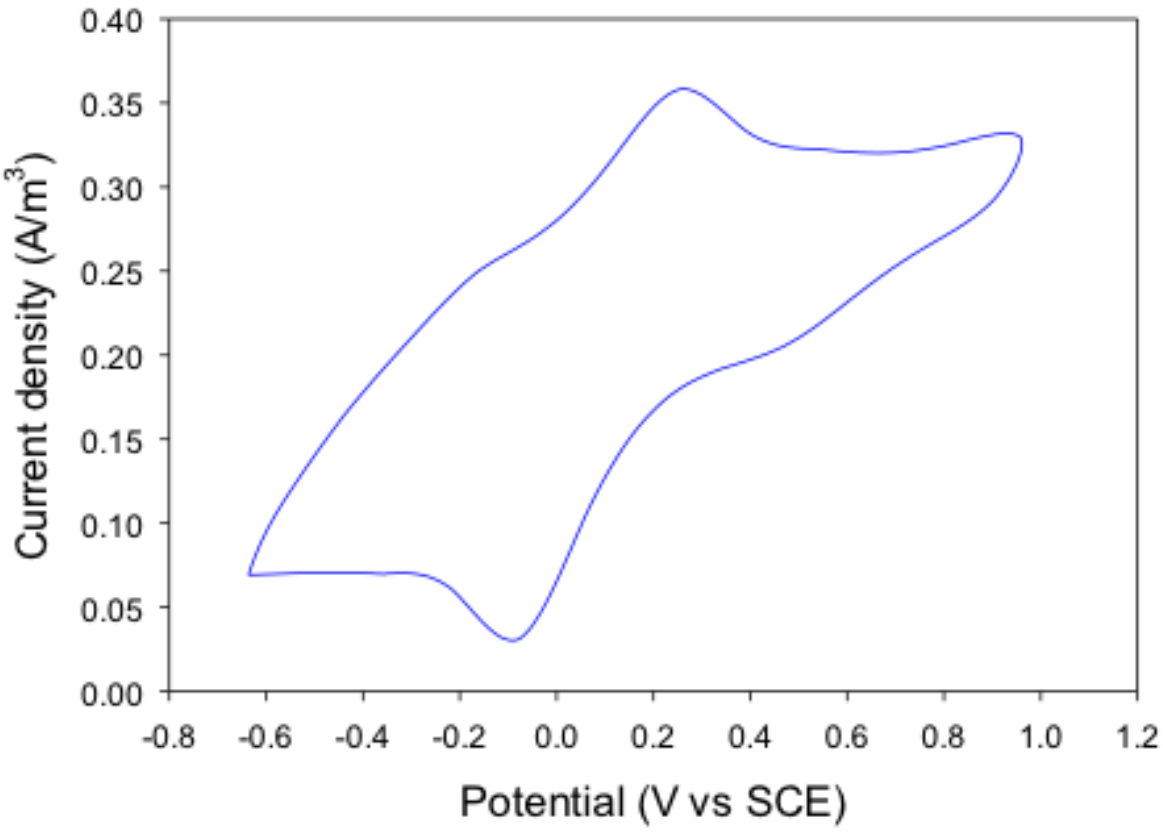

529